

Beam Pointing Optimizations for Omega Implosions

Webster Kehoe

Joseph C. Wilson Magnet High School

Rochester, New York

Advisor: Dr. R. S. Craxton

Laboratory for Laser Energetics

University of Rochester

Rochester, New York

October 2016

1. Abstract

One essential requirement for successful laser driven fusion is target uniformity during compression. To ensure high uniformity, the OMEGA laser uses 60 beams aimed at the target in a specific geometric pattern, a truncated icosahedron. However, if some beams either lose functionality or are diverted for use with diagnostics, the target uniformity is severely decreased. To remedy this issue other beams can be repointed to compensate for those that are missing. In one experiment, six beams were aimed towards a secondary target, leaving only 54 beams to drive the implosion. As a result, the root-mean-square (RMS) nonuniformity increased from 0.40% for the perfect configuration with all 60 beams, to 10.33%. Using the hydrodynamics simulation code SAGE, the beam pointings of the remaining 54 beams were manually optimized to maximize uniformity, reducing the RMS to 0.67%. Since this method of optimization is very time intensive, an effort was made to explore whether it was possible to find an acceptable configuration in a much shorter amount of time given any combination of missing beams. An algorithm was created to find the optimal configuration given any single missing beam. This algorithm produced an RMS of 0.54%, which was equal to that of the non-algorithmic optimization. The algorithm was extended to the case of multiple missing beams, and applied to the case of six missing beams. With an RMS of 0.79%, the algorithm gave results very close to the manual optimization. This could also have implications for a fusion reactor, by enabling it to automatically repoint beams if some beams go out of service or need maintenance.

2. Introduction

Nuclear fusion has significant potential for a variety of reasons. It is safe, clean, and perhaps most important, it is fully renewable, as it relies on hydrogen, the most abundant element in the universe. One method of achieving nuclear fusion is direct drive inertial confinement fusion.^{1,2} In inertial confinement fusion, laser beams are used to compress and heat a small capsule filled with fusion fuel, as shown in Fig. 1. The capsule typically consists of a thin plastic shell surrounding a shell of frozen deuterium and tritium, two isotopes of hydrogen. As the laser irradiates the capsule's outer shell it ablates material from the shell. The opposite reaction of this ablation is a force that pushes inwards, toward the center of the target. The ablation process is akin to creating a rocket, except that the rocket is spherical, with all sides of it pushing towards the center. This force creates an implosion, as the capsule collapses inward. This collapse creates extreme conditions. To produce a sufficient number of fusion reactions, temperatures must reach approximately 100 million degrees Celsius and the deuterium and tritium must have a density over 200 grams per cubic centimeter. These extreme conditions allow the two reacting nuclei to overcome their natural repulsion forces and combine to form a helium atom and a neutron, whose kinetic energy is the form of the energy being released.

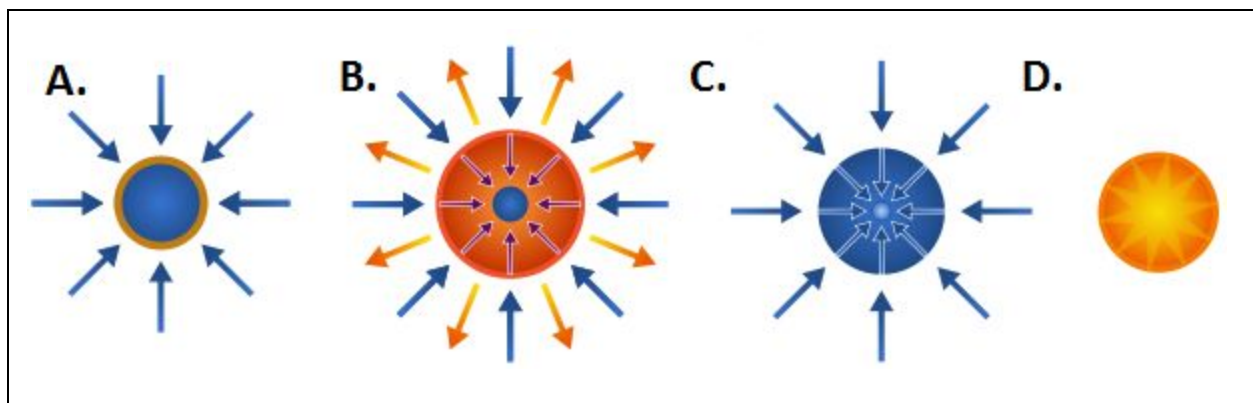
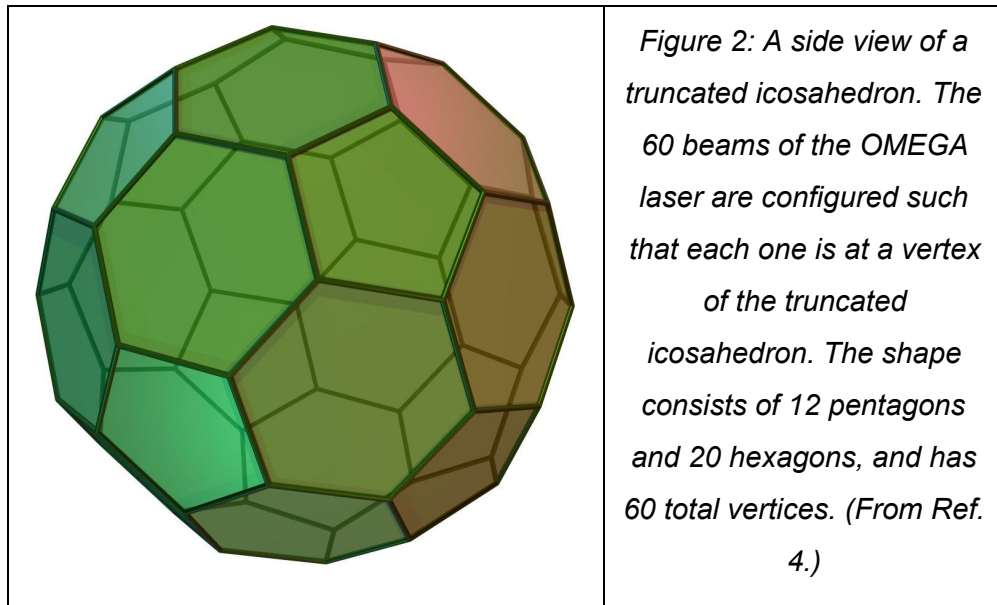


Figure 1: A diagram of the steps that occur as the laser beams compress the target. The blue arrows represent the laser irradiation, while the orange arrows represent blowoff. The blue circle represents the target. The orange ring in part A represents the plasma surrounding the target. Figure D represents the target when it reaches thermonuclear burn. (From Ref. 3.)

If the density of the fuel multiplied by the radius of the fuel is large enough, the energy from the reaction will be deposited in the fuel, initiating more reactions. This process is known

as ignition. If ignition occurs, the energy released by the fusion reactions will be greater than the energy input, which is referred to as “breakeven”. Once the energy released is 100 times that of the energy input, high energy gain will be achieved, allowing for a viable nuclear fusion reactor.



For fusion to occur, it is essential to have the beams irradiate the target uniformly. This will be a primary design criterion in future fusion reactors. The OMEGA laser uses 60 beams arrayed on the vertices of a truncated icosahedron (see Fig. 2), which resembles a soccer ball, to compress the target. The truncated icosahedron design was chosen for the OMEGA facility because it allows for a large number of beams in a symmetrical configuration.

Because of the good uniformity of the OMEGA design it may be used as the basis for a future fusion reactor. However, one problem that arises is what to do if one or more beams lose functionality. Since the region on the target where the beam is aimed no longer receives the same energy deposition as the other parts of the target, it will be less compressed. This problem also occurs in diagnostic experiments on OMEGA, in which some beams are diverted from the main implosion. In either scenario, there will be a severe drop in compression uniformity.

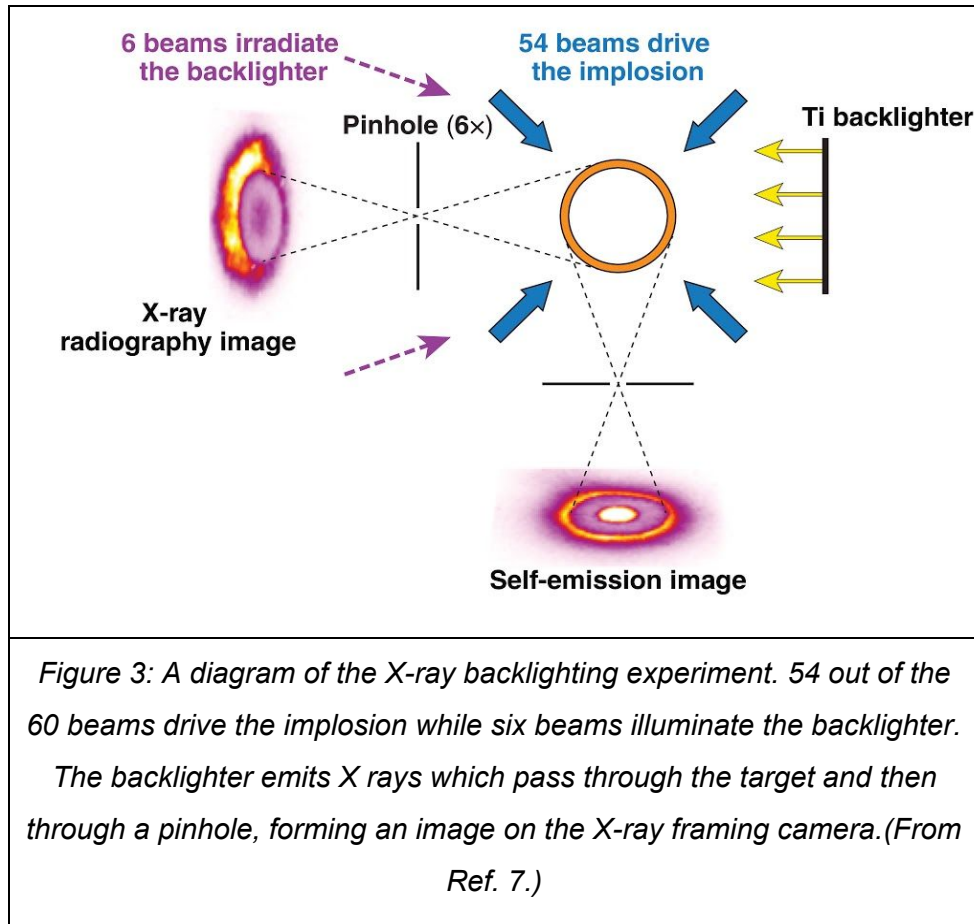
This problem can be minimized by repointing the other beams slightly towards the beams that are missing. However, the process of calculating the correct repointings can be extremely time consuming, as it is currently done through human optimization of a large number of parameters using the hydrodynamics simulation program SAGE.⁵ If an effective algorithm was developed it would significantly decrease the amount of time required to find optimal configurations when diverting beams for diagnostic experiments, as well as allow a fusion

reactor to automatically repoint beams if one beam were to fail or be out of service for maintenance. This would enable the reactor to continue to produce energy while the beam was being repaired.

In this work a configuration was greatly improved upon for a specific diagnostic experiment, and an algorithm was developed that calculates beam repointings given any combination of missing beams.

3. X-ray Backlighting Experiment

To gain more knowledge on how best to improve the compression scientists often use diagnostic experiments that allow them to see snapshots of what is going on during the compression. One common experiment is X-ray backlighting. As illustrated in Fig. 3, for an experiment carried out by T. Michel⁶ and reported in Ref. 7, some laser beams (in this experiment six) are pointed at a secondary target, which emits x rays that pass through the target to a pinhole camera on the other side. Some of the X-rays are blocked by the dense target shell. This creates an absorption image on the X-ray framing camera. The other circle below the target in Fig. 3 shows the image that is created by the self-emission of the X-rays from the hot outer plasma surrounding the target. This image is used to diagnose the shape of the implosion.



As a result of pointing the six beams away from the main implosion, the regions that the beams were previously compressing become not nearly as compressed as the rest of the sphere. The predicted non-uniformity is illustrated in Fig. 4, which is a sinusoidal projection of the energy deposition on the sphere, that displays in a similar way to oval maps of the Earth. In this case the top is the “North Pole” and the bottom is the “South Pole”. The middle horizontal line is the entire equator with the leftmost and rightmost points being the same point because it wraps around. The deep blue represents an area of much lower energy deposition compared to the rest of the sphere. The missing beams are shown by orange circles. The uneven energy deposition depicted in this projection results in a very weak uniformity of 10.33% RMS (where the Root Mean Square is the square root of the arithmetic mean of the squared nonuniformity averaged over the surface of the sphere), compared to the 0.4% RMS that can be achieved with all 60 beams in their original configuration.

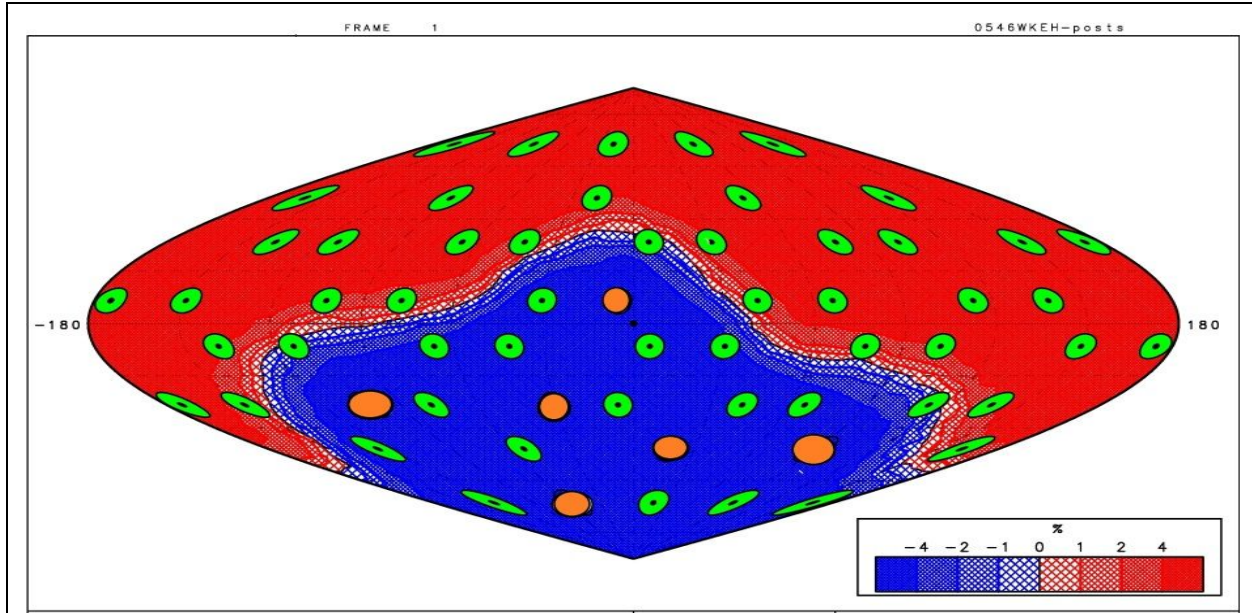


Figure 4: 2-D energy deposition profile illustrating target non-uniformity. Blue indicates areas with a lack of energy deposition whereas red indicates areas of too much energy deposition. The more intense the color, the higher the non-uniformity. The green circles represent the beam port locations on the target chamber and the small black circles indicate the positions on the target where the beams are aimed. In this case no beams have been repointed. The orange circles indicate beams that are missing. The RMS energy deposition nonuniformity in this simulation is 10.3%.

3.1 Prior Design

To compensate for the missing beams, an experiment was carried out⁷ in which some of the remaining beams were repointed towards the areas in Fig. 4 where there is not enough energy deposited. It is important to note that each beam spreads its energy over a large region on the target, with the highest absorption being at the center of the beam. The design moved only the 18 beams closest to the six missing beams. The design also took advantage of the natural tri-fold symmetry of the truncated icosahedron (see Fig. 2). Each beam repointing has two parameters, the distance it moves along a great circle of the sphere, and its direction, defined by a point on the sphere it moves towards. By utilizing the 3 fold symmetry, which is illustrated in Fig. 5, the number of parameters is reduced from 36, for all 18 beams, to just 12, for six beams. After these six beams are optimized, the same relative movements are applied to their symmetrical counterparts. In this case most of the beams moved towards the missing

beam closest to them except for the 3 beams in the central hexagon which all move toward the center.

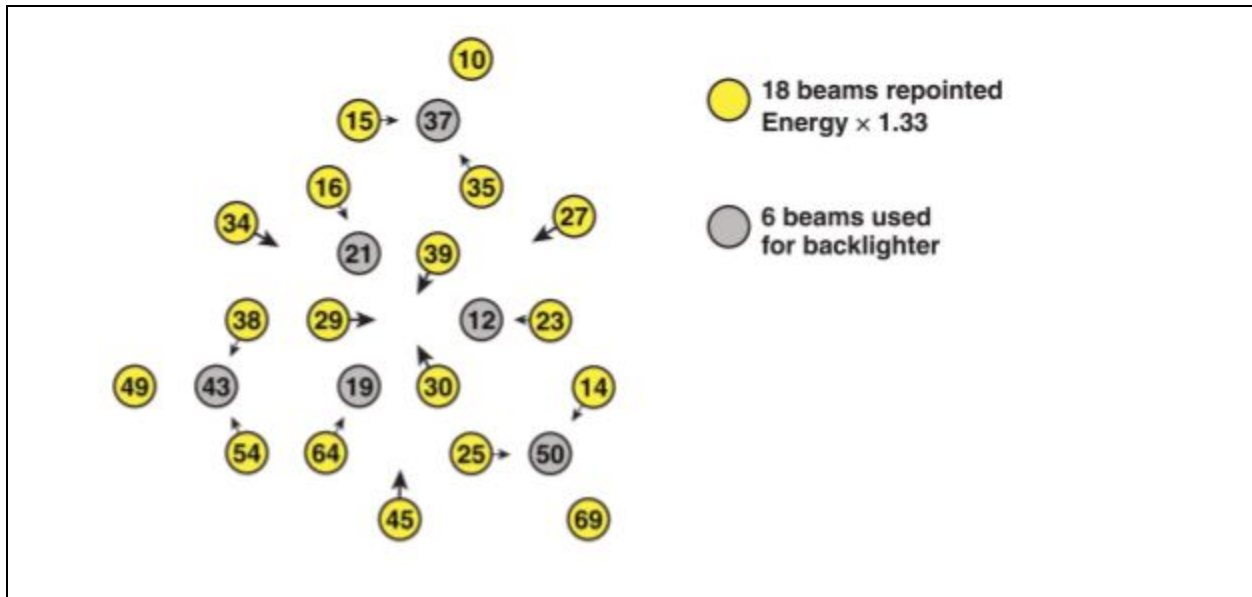
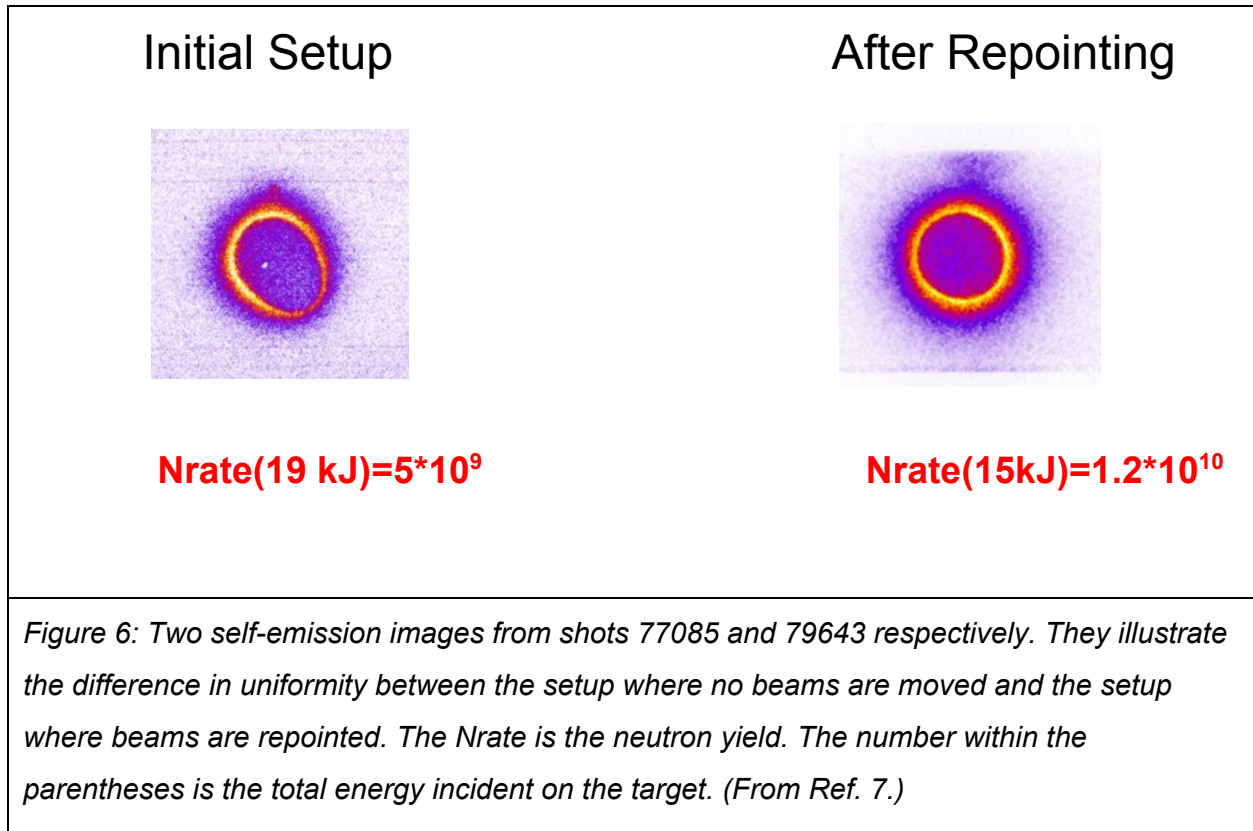


Figure 5: Flattened projection of the missing beams in the OMEGA backlighting experiment, and the 18 beams directly around them. Grey circles indicate missing beams. The number inside each circle is the designated number of each beam. The “x1.33” indicates that the beams indicated in yellow have had their relative energies multiplied by 1.33 to compensate for the missing beams. In practice, the unaltered beams were given 1/1.33x less energy. The arrows represent which direction each beam was moved in. (From Ref. 7.)

Unfortunately, merely changing the pointings of the 18 beams is not enough to compensate for the energy of the six missing beams. As a result, the 18 beams were given increased relative energies 33% higher than the other beams. However, since there is a limit on the amount of energy each laser beam can possess, and all the beams are operated at maximum energy, it is impossible to increase the energy of the 18 beams. Rather, the energy of all the other beams had to be decreased, so they were reduced to 75% energy. There is significantly better uniformity, as shown in Fig. 6.



In Fig. 6, the area of non-uniformity near the bottom right in the initial setup image corresponds directly to the area of deep blue in Fig. 4. The repointed configuration yielded very high uniformity, with a calculated RMS of only 0.74%. This high uniformity allows for a much higher neutron yield despite the fact that less energy is incident on the target (15 kJ compared to 19 kJ). The neutron yield is a key indicator of the success of the implosion. One of the primary goals of the experiment is to observe neutron yields as close as possible to the neutron yield from a full 60 beam implosion.

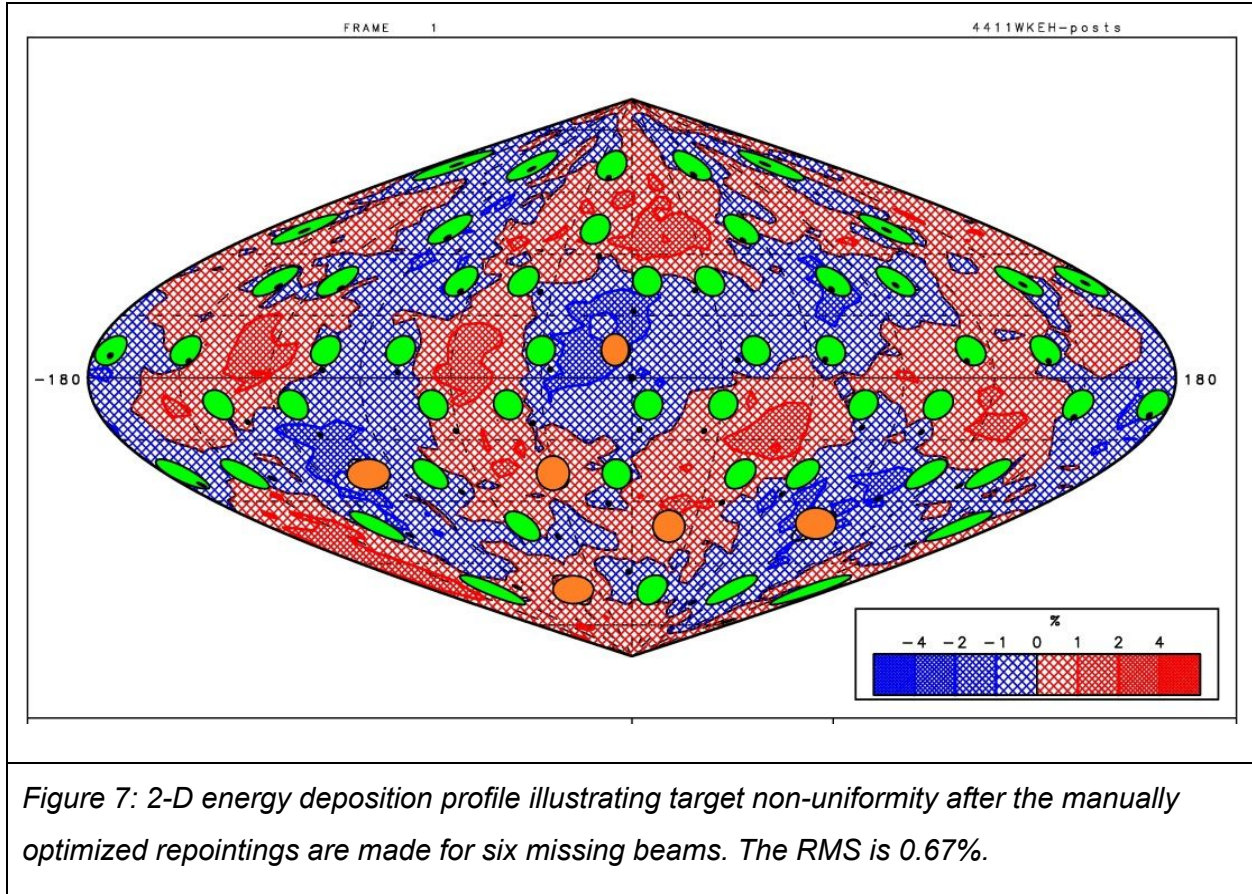
Optimally, to achieve a higher neutron yield the beam configuration needs to have strong uniformity while also depositing the full 19 kJ of energy.

3.2 Optimized Design for 6 Beams Missing

To pursue the goal of attaining the high uniformity of the previous design and also using the full 19 kJ of energy, all 54 beams were repointed, and all beams were kept on maximum energy. In the manual optimization process, a design was tested by running it through the hydrodynamics code SAGE to find the RMS value. The design was evaluated based on the sinusoidal projection of energy deposition and new pointings were input that addressed the problems of that configuration. This process was repeated until the RMS value ceased to

decrease through a large number of runs. Most of the adjustments were based on repointing the beams either directly toward a missing beam or toward the center of all the missing beams, as shown in Fig. 5. However, not all beams were pointed directly at one of those two places. Often there would be minor adjustments that directed energy towards places of low energy deposition based on the most recent sinusoidal projection. One of the major issues complicating the process is the fact that each beam is large enough that even after it is moved there will still be a large amount of energy deposited around its original area (denoted by the green circles in the energy deposition profiles). This is because the part of the beam that is hitting that area is hitting it at normal incidence, where rays experience the greatest absorption, whereas the other parts of the beam are not. Thus, the beam energy deposition profile will always trend toward its starting point. This phenomenon is part of the reason the optimizations have always been done manually.

To minimize the number of parameters this design also took advantage of the natural tri-fold symmetry, so 18 beams were repointed and the same relative repointings were applied to the other 36 beams. With each of the 18 beams having two parameters, 36 parameters had to be optimized. After hundreds of trials running various designs through SAGE the optimized design was found, shown in Fig. 7. Like all other such deposition figures used here it is on the same scale as Fig. 4. In this design almost all of the surface of the target is within 1% non-uniformity, resulting in a total RMS of 0.67%. This decrease in non-uniformity from the prior 0.74% could be due to the fact that more parameters were varied. Overall, since both designs have extremely high uniformity - the difference between the two being negligible - the largest improvement is the maximization of the total laser energy. This should result in a higher neutron yield. Because of this, the configuration will be used for future backlighting experiments.⁶



4. One Beam Missing

Beyond X-ray backlighting, there are a variety of other reasons why some number of beams would be taken out from the original configuration. In the case of a future nuclear fusion reactor, it is possible that at some time a beam would lose functionality. However, if there was a set repointing that could be applied, the reactor could continue to function, with only slightly lower neutron yield. Since every beam is equivalent in the OMEGA geometry, with each beam being at the intersection of two hexagons and a pentagon (see Fig. 2), solving for the best configuration with any missing beam will have the same solution as for any other single missing beam. With one missing beam and no adjustments made to the other 59, the RMS value is raised to 2.80% from 0.40%. After another manual optimization process (similar to the one for six missing beams) the energy deposition was extremely uniform except for a few areas of non-uniformity between 1% and 2% (see Fig. 8). The overall RMS was reduced to 0.54%.

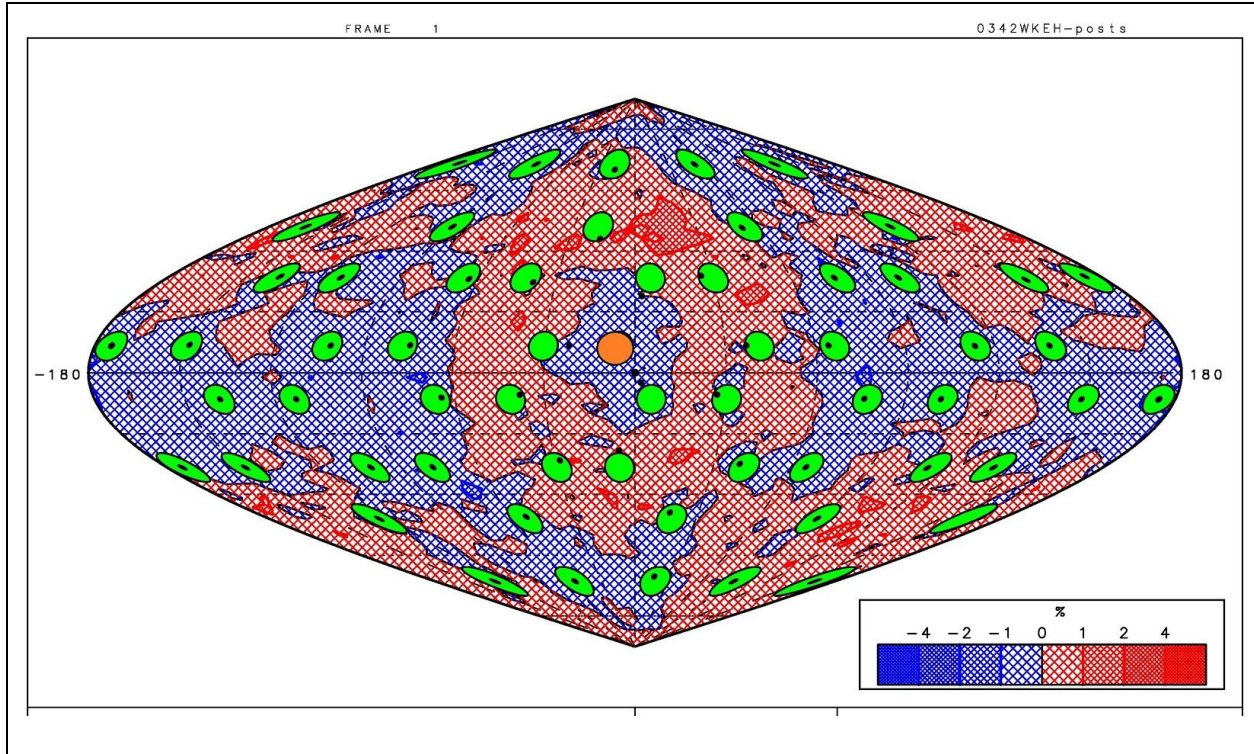


Figure 8: 2-D energy deposition profile illustrating the target non-uniformity for one beam missing after the manually optimized repointings are made. The RMS is 0.54%.

5. Developing the Algorithm

One concept that became evident through the optimization process is that there is basic logic that dictates what the optimal design will look like. The closer a beam is to a missing beam the more it will move. Also, small movements of all the beams are better than large movements of only a few. It seemed plausible that there could be a basic equation that describes how far the beams should be moved towards the missing beam. To continue with this idea, the movements toward the missing beams were graphed against the distance d between the beam and the missing beam, measured along a great circle on a unit sphere (Fig. 9). To find d the equation⁸

$$d = \arccos(\cos\theta_1 \times \cos\theta_2 \times \cos(\Phi_2 - \Phi_1) + \sin\theta_1 \times \sin\theta_2) \tag{Equation 1}$$

was used, where θ is the latitude, Φ is the longitude, and the subscripts 1 and 2 represent two beams, where 1 and 2 denote the missing beam and the beam to be moved, respectively.

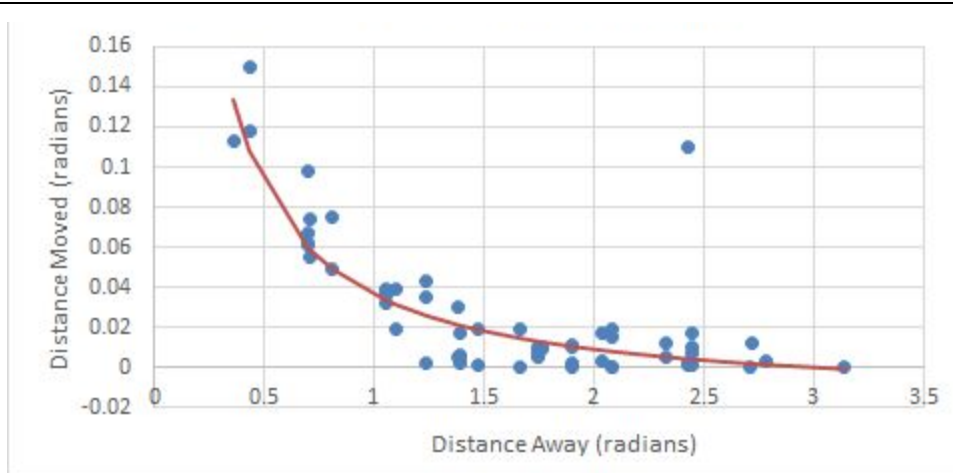
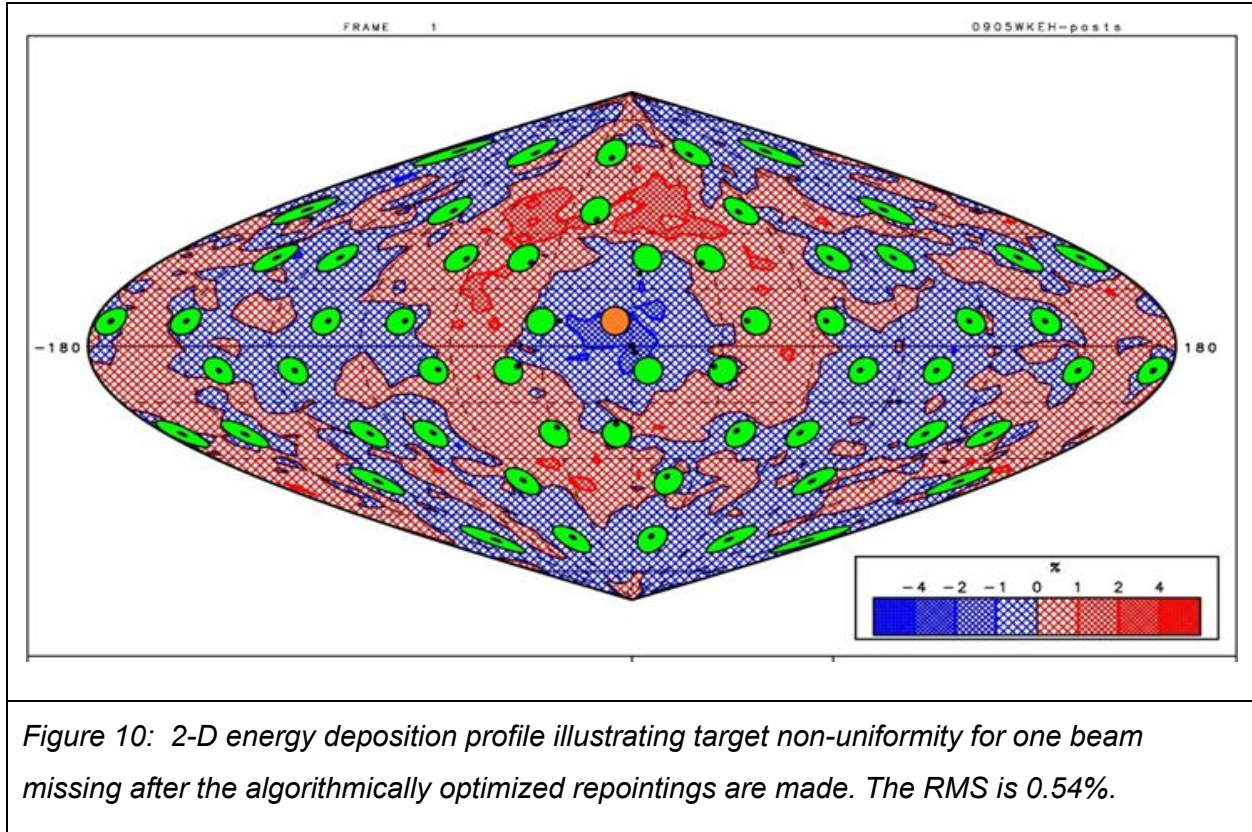


Figure 9: A graph of the distance moved (s) vs. the distance away (d) for the manual optimization. Both axes are in radians. Each blue dot indicates the values for one of the 59 beams. The red line is the trend line with the equation $s = 0.0545/d - 0.018$

The line of best fit can be approximated through the equation

$$s = A/d - B \quad (\text{Equation 2})$$

where s is the distance the beam moves toward the missing beam along the great circle connecting the two of them, and where $A = 0.0545$ and $B = 0.018$. Although there is an outlier, it is merely a result of a manual optimization decision, and since there is a high number of beams it does not have a large impact on the value of the equation coefficients. When the beam pointings were re-adjusted to follow this equation the configuration produced an extremely similar sinusoidal plot to the manually optimized one (see Fig. 10 versus Fig. 8). It also produced the same RMS value, 0.54%.



6. Extending the Algorithm

It seemed feasible that this single beam algorithm could be extended to multiple missing beams as well. A program was created to pursue this idea.

For each beam (θ_2, Φ_2) , the program calculates the distance s it would move toward one of the missing beams (θ_1, Φ_1) using equation 2. Then the new latitude θ_3 and longitude Φ_3 are found using the pair of equations⁸

$$\theta_3 = \arcsin(\sin\theta_2 \times \cos(s) + \cos\theta_2 \times \sin(s) \times \cos(\beta)) \quad (\text{Equation 3})$$

$$\Phi_3 = \Phi_2 + \text{atan2}(\sin(s) \times \sin(\beta) \times \cos\theta_2, \cos(s) - \sin\theta_2 \times \sin\theta_1)$$

where θ is the latitude, Φ is the longitude, and β is the bearing which is calculated using⁸

$$\beta = \text{atan2}(\sin(\Phi_1 - \Phi_2) \times \cos\theta_1, \cos\theta_2 \times \sin\theta_1 - \sin\theta_2 \times \cos\theta_1 \times \cos(\Phi_1 - \Phi_2)) \quad (\text{Equation 4})$$

By summing the changes in latitude and longitude for each missing beam the final latitude and longitude of the beam are found.

Using this algorithm the program is able to take any combination of missing beams and produce a suitable repointing configuration. When this algorithm was applied to the original case of six missing beams it produced a configuration with an RMS of 1.02%, shown in Fig. 11.

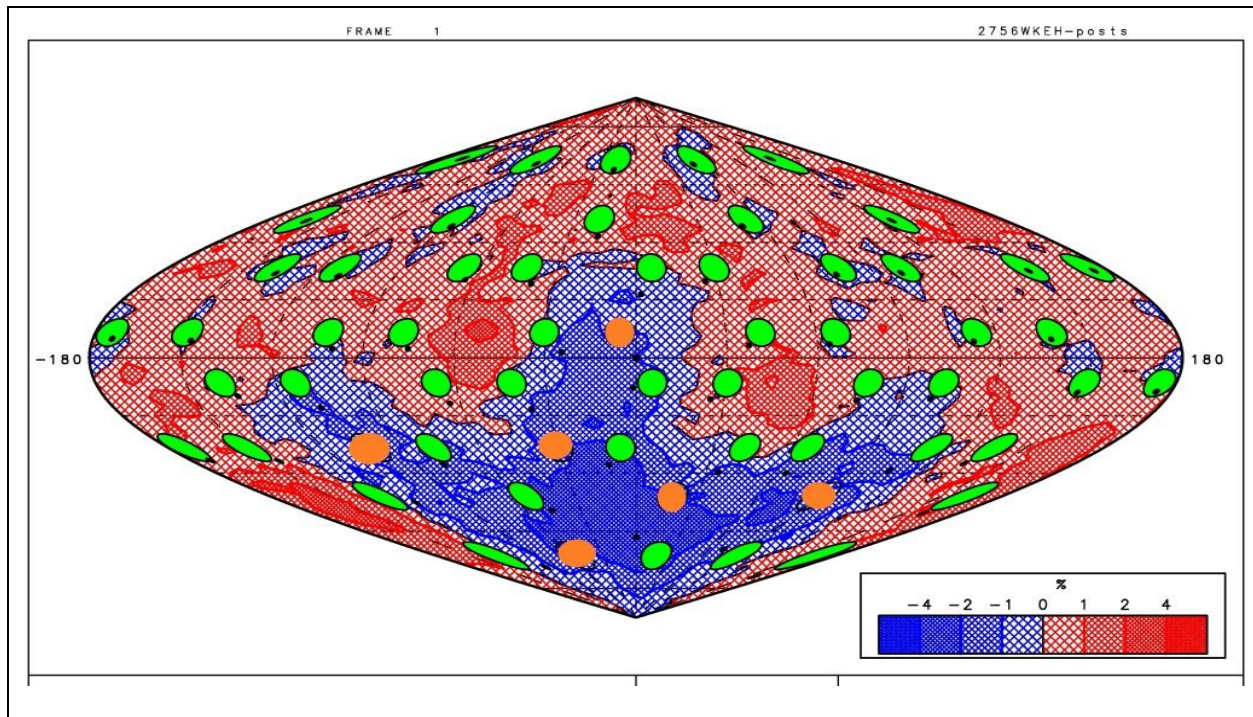
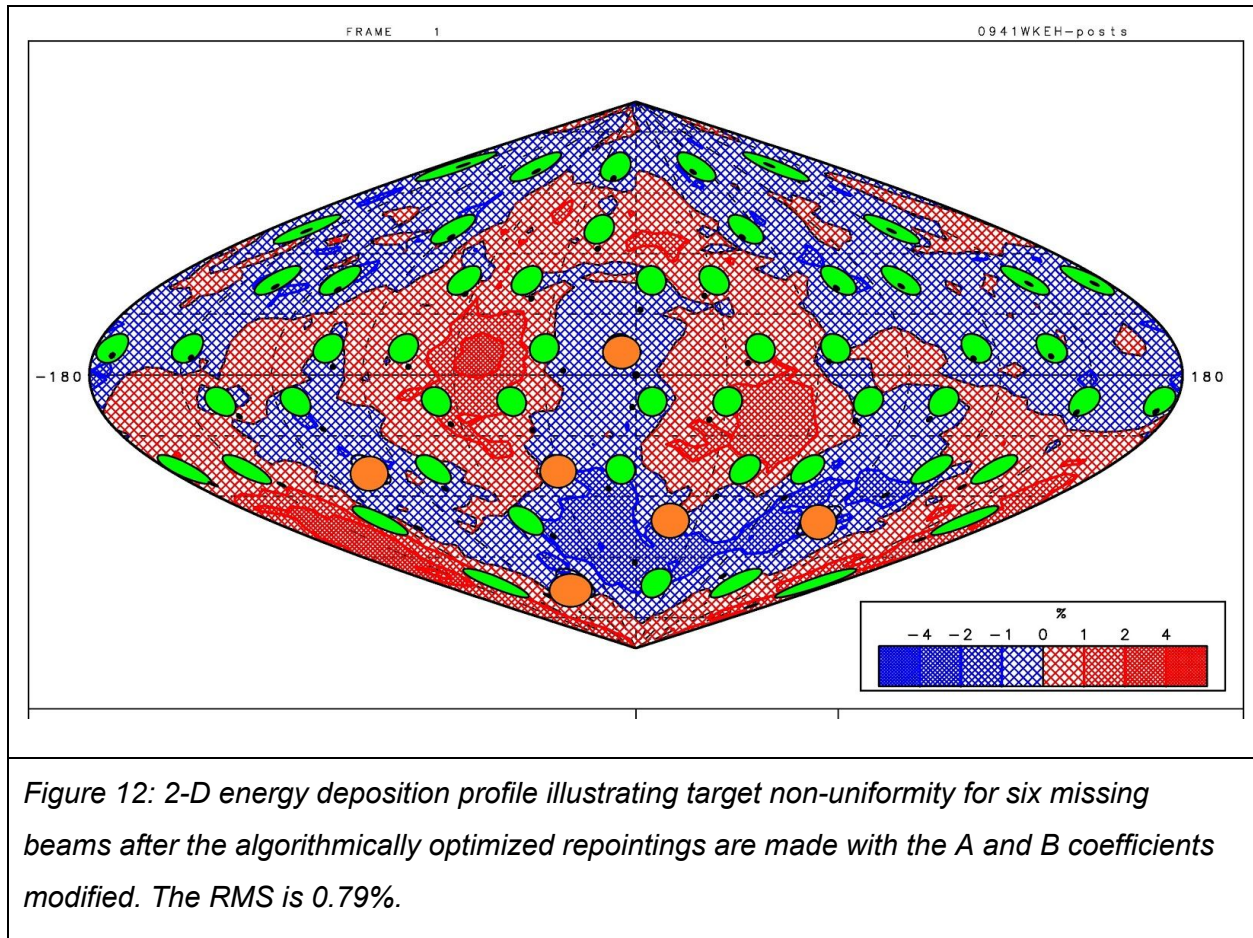


Figure 11: 2-D energy deposition profile illustrating target non-uniformity for six beams missing after the algorithmically optimized repointings were made based on Equation 2 with the original A and B coefficients. The RMS is 1.02%.

However, with the large area of lower energy deposition centered around the missing beams that is clearly visible in Fig. 11, it becomes clear that the repointings of the beams were not quite large enough. To account for this, the coefficients in the equation were changed so that each beam moved farther towards the missing beams. To find the correct coefficient values, A and B were optimized through a number of trials. However, this was a relatively quick process since there were only 2 parameters, one for each coefficient. In the optimized solution coefficient A was increased from 0.0545 to 0.0575 while coefficient B had a negligible change.

After this modification the configuration produced by the algorithm (shown in Fig.12) had an RMS of 0.79%, very close to the 0.67% of the manual optimization. By comparing the aim points (small black circles) in Fig. 12 to those in Fig. 7 one can see the similarities in the repointings, and the tri-fold symmetry is still evident. One interesting thing to note is that for both the six beam case and the one beam case the algorithm produces a configuration where there are certain areas that are much more non-uniform than the rest of the target, but the extremely

high uniformity in the remainder of the target allows the RMS value to stay about the same. The closeness of the algorithmic and manual values demonstrates the validity of the algorithm for multiple beams. This could drastically reduce the amount of time it takes to find a suitably uniform configuration when some beams are missing. For example, if 5 beams were missing with no symmetry, the 55 beams would make for a total of 110 parameters to optimize whereas with the algorithm there are only 2.



7. Future Work

To improve even further on the algorithm it would be beneficial if the program could recognize certain aspects of the pattern generated by the missing beams. One major factor that has a large effect on how far the beams should be moved is how clustered the beams are. To test out the nature of the relationship between clustering and the RMS the program was run with the original coefficient values ($A=0.0545$, $B=0.018$) for two, three, and four beams missing, each with two extreme cases, the most spread out and the most clustered.

Number of Beams	RMS when beams are most spread out	RMS when beams are most clustered
2	0.66%	0.83%
3	0.76%	1.06%
4	0.83%	1.37%

Table 1: RMS values of configurations generated by the algorithm with the base coefficients for two, three, and four beams for the two extreme cases of the missing beams being most spread out or most clustered.

The results are summarized in Table 1. Currently, with the base algorithm the program gives worse results when the beams are clustered, demonstrating that it could be beneficial to have coefficient A increase to account for the beams not moving enough in those cases.

Through analyzing these relationships it may be possible to have the program recognize these patterns and choose the appropriate coefficient values accordingly. This would eliminate all human optimization from the process and decrease the time needed for repointing calculations even further.

8. Conclusion

In conclusion, an optimal six beam configuration was found for an X-ray backlighting experiment on OMEGA. This configuration had an RMS of 0.67% and improved on the previous design by not requiring the energy to be reduced on any beams. An optimal configuration for any single missing beam was also created, and had an RMS of 0.54%. An algorithm was developed for the case of one missing beam and yielded the same RMS value. This algorithm was extended to be able to produce a suitable configuration given any number of missing beams. The algorithm was tested on the original six beam case and had an RMS of 0.79%, extremely close to the 0.67% of the manually optimized configuration. However, the manual method had 36 separate parameters while the algorithmic optimization only had 2, making it much more time efficient. This time savings is even more apparent when there is a set of missing beams with no symmetry, where there would likely be over 100 parameters to optimize if it were to be done manually.

Overall, it appears that the algorithm allows suitable configurations for a wide range of combinations of missing beams with limited human input. The algorithm could be very beneficial for a future reactor that could automatically repoint if one or more of the beams were to lose functionality.

9. Acknowledgements

First, I would like to thank Roger Janezic for telling me about the Summer High School Program at the Laboratory for Laser Energetics and encouraging me to apply. I would also like to thank the Laboratory for providing this program and making this opportunity possible. Most of all, I would like to thank Dr. R. Stephen Craxton for being extremely helpful and supportive as my advisor, and for running the entire program.

10. References

1. J. Nuckolls, L. Wood, A. Thiessen, and G. Zimmerman, "Laser compression of matter to super-high densities: Thermonuclear (CTR) applications," *Nature*, vol. 239, p. 139, 1972.
2. R.S Craxton et al., "Direct-drive inertial confinement fusion: A review," *Physics of Plasmas*, vol. 22, p. 110501, 2015.
3. B.D. Esham, Inertial Confinement Fusion. Digital image. Wikipedia. N.p., 5 July 2007. Web. 10 Sept. 2016.
4. Truncated Icosahedron. Digital image. Wikipedia. N.p., 22 May 2005. Web. 10 Sept. 2016.
5. R.S. Craxton and R. L. McCrory, "Hydrodynamics of thermal self-focusing in laser plasmas", *Journal of Applied Physics*, vol. 56, p. 108, 1984.
6. T. Michel, private communication.
7. R.S. Craxton, M. Hohenberger, W. Kehoe, F.J. Marshall, D.T. Michel, P.B. Radha, M.J. Rosenberg, *Bulletin of the American Physical Society*, Vol. 61, p. 231, 2016.
8. C. Veness, www.movable-type.co.uk. "Movable Type Scripts." Calculate Distance and Bearing between Two Latitude/Longitude Points Using Haversine Formula in JavaScript. MIT, 2002. Web. 12 Nov. 2016.